

The Self-Trapping Line of the Holstein Molecular Crystal Model in One Dimension

A. H. Romero^{1,3}, David W. Brown² and Katja Lindenberg³

¹ Department of Physics,

University of California, San Diego, La Jolla, CA 92093-0354

² Institute for Nonlinear Science,

University of California, San Diego, La Jolla, CA 92093-0402

³ Department of Chemistry and Biochemistry,

University of California, San Diego, La Jolla, CA 92093-0340

(October 20, 2019)

The ground state of the Holstein molecular crystal model in one dimension is studied using the Global-Local variational method, analyzing in particular the total energy, kinetic energy, phonon energy, and interaction energy over a broad region of the polaron parameter space. Through the application of objective criteria, a unique curve is identified that simply, accurately, and robustly locates the self-trapping transition separating small polaron and large polaron behavior.

PACS numbers: 71.38.+i, 71.15.-m, 71.35.Aa, 72.90.+y

I. INTRODUCTION

The self-trapping transition is the core conundrum of polaron theory. Though this transition is expected to be smooth at finite parameter values, there exists nonetheless a strong feature in the intermediate-coupling regime that separates states that are predominantly "small-polaron-like" from states that are predominantly "large-polaron-like". This feature, while not in itself singular, is related to singular behavior in the adiabatic limit and appears to influence perturbation theory much as more straightforwardly-understood singularities affect other expansions; i.e., weak-coupling perturbation theory [1–3] breaks down as this feature is approached from below, and strong-coupling perturbation theory [3–9] breaks down as this feature is approached from above.

Our investigations here are motivated in part by the following observation: Much as a discrete curve (e.g., the unit circle) may describe a limited domain of convergence for a series representation of a function though the function itself may be well-behaved over most of that curve, there is meaning to the notion of a discrete line describing the location of the self-trapping transition though the physical phenomenon we study may be smooth throughout the finite parameter space. However, lacking absolute knowledge of the underlying self-trapping phenomenon, we must necessarily proceed more empirically and attempt to *infer* the location of a unique self-trapping line from limited observations of polaron properties. From such observations on numerous distinct quantities over large regions of the polaron parameter space, we conclude that the self-trapping line of the Holstein model in one dimension is accurately and robustly described by the simple relation

$$g_{ST} = 1 + \sqrt{J/\hbar\omega} , \quad (1)$$

in which J is the nearest-neighbor electronic hopping integral, ω is the Einstein frequency, and g is the dimensionless coupling strength. This curve could already be inferred roughly in Figure 4 of Ref. [10], but here we are led to this functional form by direct, high-precision numerical study.

Describing the self-trapping transition with accuracy clearly requires methods that are *non-perturbative*. In recent years, several methods have been developed that are capable of describing the intermediate-coupling regime with high accuracy over non-trivial ranges of adiabaticity; most importantly to our present purposes are the Global-Local variational method [10–12], the density matrix renormalization group method [2,13], and cluster diagonalization methods [7,14–19]. Elsewhere, we have made direct quantitative comparison of these quite independent methods, demonstrating their agreement to multiple significant digits, not only in the value of the polaron ground state energy, but across the entire Brillouin zone. Here, we use the Global-Local variational method on periodic lattices of 32 sites, supported by low orders of perturbation theory on infinite lattices. Details about the numerical method can be found in Ref [10].

We focus on the 1-D Holstein Hamiltonian [20,21]

$$\hat{H} = \hat{H}_{kin} + \hat{H}_{ph} + \hat{H}_{int} , \quad (2)$$

$$\hat{H}_{kin} = -J \sum_n a_n^\dagger (a_{n+1} + a_{n-1}) , \quad (3)$$

$$\hat{H}_{ph} = \hbar\omega \sum_n b_n^\dagger b_n , \quad (4)$$

$$\hat{H}_{int} = -g\hbar\omega \sum_n a_n^\dagger a_n (b_n^\dagger + b_n) , \quad (5)$$

in which a_n^\dagger creates a single electronic excitation in the rigid-lattice Wannier state at site n , and b_n^\dagger creates a quantum of vibrational energy in the Einstein oscillator at site n .

II. CHARACTERISTIC ENERGIES

The global ground state energy E_0 is composed of contributions from the three principal components of the total Hamiltonian:

$$E_0 = \langle \psi | H | \psi \rangle = E_{kin} + E_{ph} + E_{int} , \quad (6)$$

in which E_{kin} is the kinetic energy, E_{ph} is the phonon energy, and E_{int} is the electron-phonon interaction energy.

Our numerical results for these quantities are summarized in Figure 1 as functions of the electron-phonon coupling strength for several values of $J/\hbar\omega$. Each curve in

Figure 1 contains 80-200 data points, each figure panel collectively representing more than 1100 distinct polaron ground states. No smoothing has been performed; each "curve" is a polygonal arc connecting computed energies.

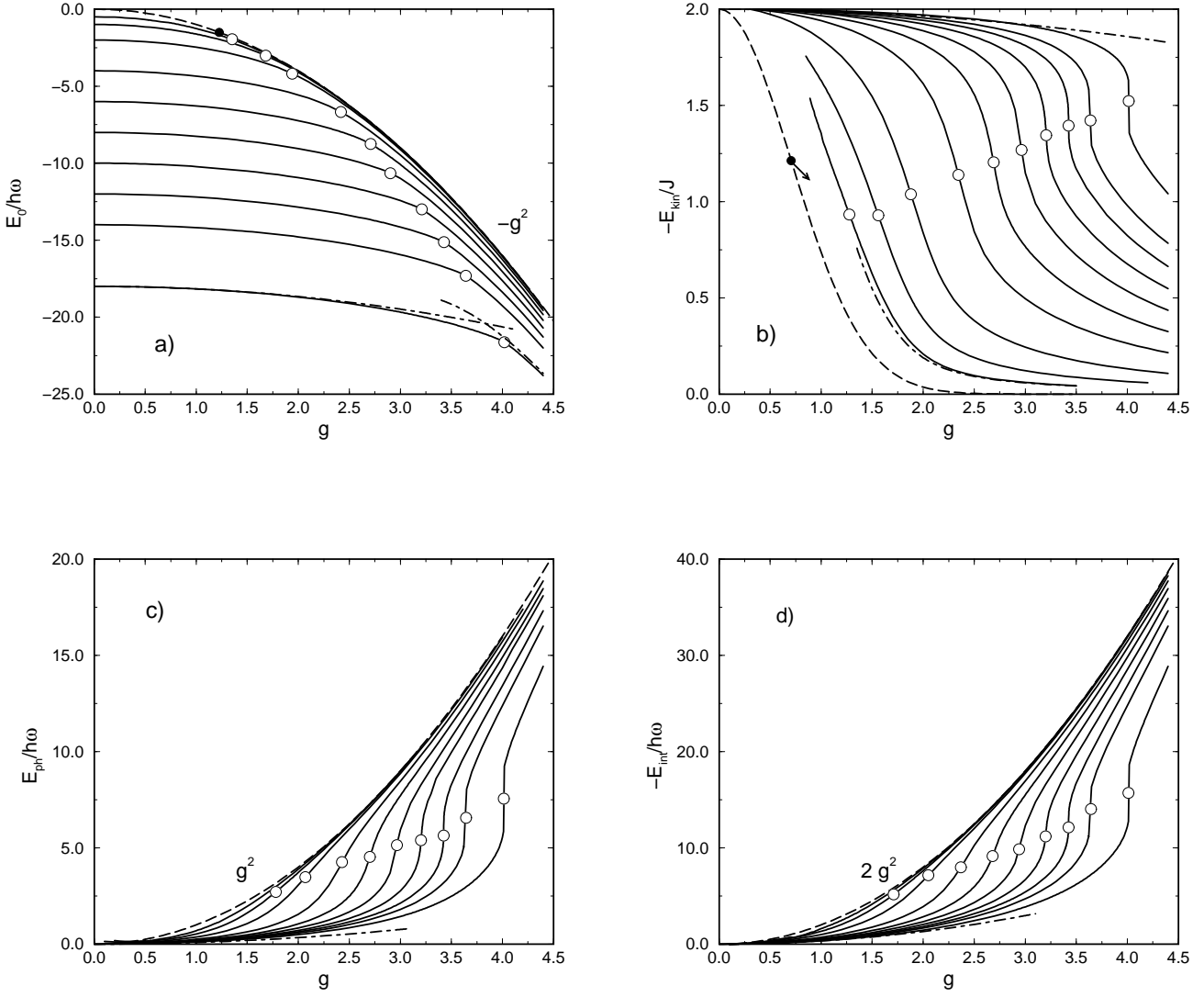


FIG. 1. The ground state energy E_0 (a) and its several components E_{kin} (b), E_{ph} (c), and E_{int} (d) as functions of the electron-phonon coupling for $J/\hbar\omega = 0.25, 0.5, 1.0, 2.0, 3.0, 4.0, 5.0, 6.0, 7.0$ and 9.0 (solid curves, top to bottom in (a), left to right in (b), (c), and (d)). The dashed curve in each figure panel is the exact $J \rightarrow 0$ limit appropriate to each case. The chain-dotted curves illustrate Eqs. (7) - (11) for $J/\hbar\omega = 9$, and (12) for $J/\hbar\omega = 1/4$. Circles (○) indicate the "break" in each energy curve associated with the self-trapping transition. Bullets (●) in (a) and (b) indicate the exact $J = 0$ termini of the self-trapping lines appropriate to E_0 and E_{kin} as determined from Eqs. (11) and (12), respectively. The arrow in (b) indicates the exact initial slope of the E_{kin} self-trapping line as determined from Eq. (12).

Although the aggregate (E_0) of these several contributions is subject to variational constraint, the values of the separate contributions (E_{kin} , E_{ph} , E_{int}) are not; in principle, the latter are vulnerable to distortions that may misrepresent some aspects of ground state structure while still yielding favorable results for the ground state

energy. It is for such reasons that in the course of developing our method and in using it to obtain new results, we pay close attention to the detail of overall polaron structure and compare multiple quantities with known results available from independent approaches.

In the appropriate regimes, the energy contributions shown in Figure 1 are in excellent agreement with the weak-coupling perturbation theory results (Rayleigh-Schrödinger, $\hat{H}_0 = \hat{H}_{kin} + \hat{H}_{ph}$, $\hat{H}' = \hat{H}_{int}$)

$$E_0^{WC} = -2J - g^2 \frac{\hbar\omega}{\sqrt{1 + 4J/\hbar\omega}}, \quad (7)$$

$$E_{kin}^{WC} = -2J + g^2 \frac{2J}{(1 + 4J/\hbar\omega)^{3/2}}, \quad (8)$$

$$E_{ph}^{WC} = g^2 \left[\frac{\hbar\omega}{\sqrt{1 + 4J/\hbar\omega}} - \frac{2J}{(1 + 4J/\hbar\omega)^{3/2}} \right], \quad (9)$$

$$E_{int}^{WC} = -g^2 \frac{2\hbar\omega}{\sqrt{1 + 4J/\hbar\omega}}, \quad (10)$$

and with the strong-coupling perturbation theory results (Rayleigh-Schrödinger following the Lang-Firsov transformation, $\hat{H}_0 = \hat{H}_{ph} + \hat{H}_{int}$, $\hat{H}' = \tilde{H}_{kin}$)

$$E_0^{LF} = -g^2 \hbar\omega - 2J e^{-g^2} - \frac{2J^2}{\hbar\omega} e^{-2g^2} [f(2g^2) + f(g^2)], \quad (11)$$

$$E_{kin}^{LF} = -2J e^{-g^2} - \frac{4J^2}{\hbar\omega} e^{-2g^2} [f(2g^2) + f(g^2)], \quad (12)$$

$$f(y) = \text{Ei}(y) - \gamma - \ln(y), \quad (13)$$

where γ is the Euler's constant and $\text{Ei}(y)$ is the exponential integral. (We note that although this approach is commonly characterized as "strong-coupling" perturbation theory, it is actually more broadly valid. In particular, the results (11) and (12) are valid for all g if $J/\hbar\omega$ is sufficiently small, a fact that will figure in the conclusions of the next section.) One sample curve representing each of Eqs. (7) - (12) has been included in Figure 1 to illustrate this agreement. More detailed discussion and comparisons with other theories have been given elsewhere [12].

While this mutual consistency among limiting results is satisfying, the quantitative accuracy of both weak- and strong-coupling perturbation theory is superceded by that of the Global-Local method at intermediate coupling where the self-trapping transition is found; thus, we rely exclusively upon our variational method for locating the transition.

III. SELF-TRAPPING LINE

The self-trapping transition is typically resolved through a quantifiable feature that grows increasingly sharp with increasing $J/\hbar\omega$. In view of the smoothness

of the physical self-trapping transition, however, there is no reason to expect the transition to be manifested in exactly the same way in distinct physical quantities; thus, we expect an intrinsic ambiguity in the precise location of the the self-trapping transition that is diminished only by the progressive sharpening of the underlying physical phenomenon.

Since each of the displayed energies exhibits a “knee” or “break” that clearly separates distinct weak- and strong-coupling trends, any one of E_0 , E_{kin} , E_{ph} , or E_{int} could be used to locate the self-trapping effect. As objective criteria for locating this transition, we associate the transition with the particular coupling strength in the intermediate regime where each energy changes *most rapidly* with respect to g at fixed $J/\hbar\omega$; these points are identified by zeros in the second derivatives with respect to g of E_{kin} , E_{ph} , and E_{int} , and in the third derivative of E_0 as collected in Figure 2.

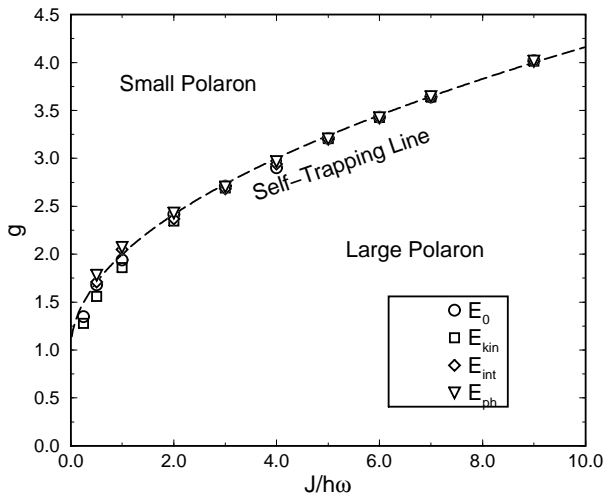


FIG. 2. Polaron phase diagram, showing the location of the self trapping transition. Discrete symbols correspond to our numerical determinations, the dashed line corresponds to the empirical curve $g_{ST} = 1 + \sqrt{J/\hbar\omega}$; no fit has been performed to obtain this curve.

These criteria amplify numerical errors and therefore are quite demanding of numerical precision. Over the interval where the transition was sought, we used a sampling interval Δg sufficiently small that directly-computed g -values alone would suffice to convey the message of Figure 2. However, as our convergence criterion, we required sufficient smoothness in the computed derivatives that the determining zeros could be interpolated with certainty considerably smaller than Δg in most cases. While this degree of precision is not really necessary to convincingly locate the self-trapping line, we applied to our study the further “check” that the collection of numerically-determined self-trapping points

should describe sensible curves through the actual family of energies as presented in Figure 1. This proves to be a stringent error criterion, since the numerical errors already amplified by repeated differentiation with respect to g are further amplified by the characteristic steepness of E_{kin} , E_{ph} , and E_{int} in the vicinity of the transition. It is especially significant, therefore, that the numerically-determined self-trapping loci obtained from E_{kin} not only describe a "sensible" curve, but appear to connect smoothly with the exactly ascertainable trend as $J \rightarrow 0$ (See Figure 1b).

Such considerations permitted a clear resolution of the self-trapping transition for most hopping integral values used in this work, with a characteristic deterioration of precision at small $J/\hbar\omega$ and g here affecting primarily $J/\hbar\omega < 1$ and $g < 1.5$. For this reason, no self-trapping loci are reported for E_{ph} and E_{int} at $J = 1/4$.

Though precision deteriorates at small $J/\hbar\omega$, the dispersion among estimated self-trapping locations that is evident in Figure 2 at smaller $J/\hbar\omega$ values is *not* the result of numerical errors, but reflects the intrinsic ambiguity in the assignment of a sharp location to a smooth transition. Using perturbation theory (See (11) and (12)), for example, one can show that as $J/\hbar\omega \rightarrow 0$, the trend in the kinetic energy criterion leads to $g = \frac{1}{\sqrt{2}}$, consistent with the trend in the E_{kin} data, while the trend in the ground state energy criterion leads to $g = \sqrt{\frac{3}{2}}$, consistent with the trend in the E_0 data. This intrinsic non-coincidence implies that there is no single line consistent with *all* of the criteria that might legitimately be considered to locate the transition. Thus, the function (1) appears to describe the *common* or *criterion-independent* trend line about which distinct locators are tightly clustered with a spread that narrows steadily in both relative and absolute terms with increasing adiabaticity.

This can be contrasted with another asymptotically-correct characterization of the self-trapping transition that follows from strong-coupling theory, namely $\lambda = \lambda_c$, where $\lambda = g^2/2J$ and $\lambda_c = \frac{1}{2}$. The difference (in g) between the latter self-trapping criterion and the one evident in our numerical data is always of order unity in absolute terms even in the adiabatic limit, and in relative terms approaches the accuracy evident across Figure 2 only for $J/\hbar\omega$ vastly larger than those investigated.

Our conclusion that the relation (1) accurately and robustly describes the location of the self-trapping transition in the Holstein model is borne out as well in the behavior of other physical quantities not presented here. Particularly important among these is the polaron effective mass, both because it is a widely-recognized hallmark of the self-trapping transition and because it expands the scope of investigation beyond the ground state. Related results for the polaron effective mass, energy band, and spatial structure will be presented elsewhere.

ACKNOWLEDGEMENT

This work was supported in part by the U.S. Department of Energy under Grant No. DE-FG03-86ER13606.

- [1] A. B. Migdal, Sov. Phys. JETP **34**, 996 (1958).
- [2] E. Jeckelmann and S. R. White, Phys. Rev. B **57**, 6376 (1998).
- [3] A. H. Romero, D. W. Brown, and K. Lindenberg, in preparation (1998).
- [4] S. V. Tyablikov, Zh. Eksp. Teor. Fiz. **23**, 381 (1952).
- [5] I. G. Lang and Y. A. Firsov, Sov. Phys. JETP **16**, 1301 (1963).
- [6] A. A. Gogolin, Phys. Stat. Sol. (b) **109**, 95 (1982).
- [7] F. Marsiglio, Physica C **244**, 21 (1995).
- [8] W. Stephan, Phys. Rev. B **54**, 8981 (1996).
- [9] M. Capone, W. Stephan, and M. Grilli, Phys. Rev. B **56**, 4484 (1997-II).
- [10] D. W. Brown, K. Lindenberg, and Y. Zhao, J. Chem. Phys. **107**, 3179 (1997).
- [11] A. H. Romero, D. W. Brown, and K. Lindenberg, submitted to Phys. Rev. B (1998).
- [12] A. H. Romero, D. W. Brown, and K. Lindenberg, submitted to J. Chem. Phys. (1998).
- [13] S. R. White, Phys. Rev. Lett. **69**, 2863 (1992).
- [14] F. Marsiglio, Phys. Lett. A **180**, 280 (1993).
- [15] A. S. Alexandrov, V. V. Kabanov, and D. E. Ray, Phys. Rev. B **49**, 9915 (1994).
- [16] A. S. Alexandrov and S. N. Mott, *Polarons & Bipolarons* (World Scientific, London, 1995).
- [17] G. Wellein, H. Röder, and H. Fehske, Phys. Rev. B **53**, 9666 (1996).
- [18] H. Feshke, J. Loos, and G. Wellein, Z. Phys. B **104**, 619 (1997).
- [19] G. Wellein and H. Fehske, Phys. Rev. B **56**, 4513 (1997).
- [20] T. Holstein, Ann. Phys. **8**, 325 (1959).
- [21] T. Holstein, Ann. Phys. **8**, 343 (1959).